

Effect of P on the hardness temperature resistance of nanostructured Ni-W electrodeposited coatings

*M J.L. Gines, M. J. Loureiro, F.J. Williams
REDE-AR, SIDERCA-TENARIS, Department of Surface Chemistry and
Coatings
Dr. Simini 250, B2804MHA, Campana, BA, Argentina*

The development of electrodeposited coatings with enhanced properties is nowadays focused on nanotechnology. More specifically, the development of temperature resistant hard coatings for a wide variety of applications is gaining attention.

Hard chromium coatings electrodeposited from hexavalent plating baths are widely used for improving hardness, wear resistance and decorative appearance of engineering tools and components despite the serious health and environmental problems they cause. Therefore, researchers have been looking for adequate replacements of Cr-based coatings.

Nanostructured Ni-W coatings are one of the potential replacements that have been extensively studied. In this work, we investigated the mechanical properties temperature dependence of electrodeposited Ni-W and Ni-W-P coatings. Changes in composition were controlled by changing the P concentration in the plating bath. The presence of P improves the mechanical properties temperature resistance of the electrodeposited Ni-W coatings.

For more information contact:

Dr. Marcelo Gines

SIDERCA-TENARIS-CINI

Dr. Simini 250

B2804MHA, Campana

ARGENTINA

Phone: 54 3489 433100 ext 34521

Fax: 54 3489 427928

E-mail: mgines@tenaris.com

1. Introduction

Hard chromium coatings based on hexavalent Cr are widely used for improving hardness, wearability, erosion resistance and decorative appearance of engineering tools and components¹⁻⁵, despite the potentially serious health and environmental problems they cause⁶. Therefore, there has been a considerable effort to find adequate replacements of Cr and Cr-based coatings to eliminate the use of hexavalent Cr.

Alternatives that have already been investigated include cobalt-based and nickel-based coatings⁷. Ni-W coatings are one of the replacements that have been extensively analyzed, because they have unique combination of tribological, mechanical, magnetic, electrical, and electro-erosion properties⁷⁻⁹. One of the drawbacks Ni-W coatings have for some tooling application is that the microhardness decreases when heating at temperatures used in some tooling applications. It is therefore desirable to improve this behavior.

Addition of small amounts of W (3.5 at.%) to electroless Ni-P (82 Ni at.% - 14.5 P at.%) coatings enhanced the thermal stability and mechanical properties for the ternary Ni-P-W systems¹⁰. Ni-P-W multilayered alloy coatings with layer thicknesses ranging from 8 to 4200 nm obtained by pulse plating showed an increase in hardness in the 500-600°C range, which decreases as the annealing temperature increases^{11,12}. Given that adding small amounts of phosphorous improved the hardness temperature resistance of Cr-based coatings¹³, it is worth studying its effect on Ni-W coatings.

In this work we electrodeposited uniform Ni-W-P coatings using NaH₂PO₂ as a source for P. Coatings with grain sizes in the nanometer range were obtained employing Bipolar Pulsed Current (BPP)¹⁴. In this method a reverse pulse selectively removes atoms with the highest oxidation potential from the deposit inhibiting grain growth during electrodeposition^{14,15}. Therefore changes in coating composition and hence in average grain sizes were controlled by changes in the current density of reverse pulses and changes in the P concentration in the plating bath. The effect of temperature on the coatings microhardness was analyzed as a function of P content. We found that adding small quantities of P increases the microhardness temperature resistance of Ni-W coatings significantly. Furthermore, improved Ni-W-P coatings have better microhardness temperature resistance than hard chromium coatings.

2. Experimental Procedures

2.1 Electrodeposition and thermal treatment

Ni-W and Ni-W-P were deposited on steel plates using the electroplating bath shown in Table 1 with NaH₂PO₂·H₂O as a source of P. Electrodeposition was carried out in an 800 mL (0.211 gal) jacketed glass cell containing the electroplating bath, which was agitated using a magnetic stirrer and heated to a temperature of 75 °C (167 °F) using a thermostatic heating bath. Carbon steel with an exposed surface area of 15 cm² (2.34 in²) was the cathode, which was separated by about 3.5 cm (0.54 in²) from a Pt mesh anode.

Prior electrodeposition steel cathodes were thoroughly cleaned using the following procedure: (1) ultrasound in an aqueous solution of 20% Extran, (2) electrolytic treatment (0.3 A/cm^2 (1.93 A/in^2) for 2 min) using a 23.2 g/L (3.10 oz/gal) aqueous solution of NaOH, (3) immersion in an aqueous solution of H_2SO_4 (10%) for 15 s.

Table 1. Bath composition used to electrochemically deposit Ni-W-P.

Bath constituent	Concentration [M]	Function
$\text{NiSO}_4 \cdot 6\text{H}_2\text{O}$	0.06	Source of Ni
$\text{Na}_2\text{WO}_4 \cdot 2\text{H}_2\text{O}$	0.14	Source of W
$\text{NaH}_2\text{PO}_2 \cdot \text{H}_2\text{O}$	0.0024 - 0.472	Source of P
$\text{Na}_3\text{C}_4\text{H}_5\text{O}_7 \cdot 2\text{H}_2\text{O}$	0.5	Ni and W complexer
NH_4Cl	0.5	Current efficient increaser
NH_4OH	As needed	pH stabilizer

The cathodic pulses used to deposit Ni-W-P coatings were run for 20 ms with a current density of 0.2 A/cm^2 (1.29 A/in^2) while anodic pulses were run for 3 ms with a current density of 0.05 A/cm^2 (0.32 A/in^2). Pulses for Ni-W-P deposition were similar but anodic pulses were maintained at 0.05 A/cm^2 (0.32 A/in^2).

2.2 Characterization techniques

The surface morphology and polished cross-sections of the as-deposited and annealed samples were characterized by scanning electron microscopy (SEM) using a XL 30 Philips equipment. Semi-quantitative chemical composition was determined by calibrated energy dispersive x-ray spectroscopy (EDS). Thicknesses were directly measured on metallurgically-prepared cross-sections of the electrodeposits using SEM images.

X-ray diffraction (XRD) was employed to determine the coatings microstructure. XRD patterns were collected at room temperature in a Phillips X'Pert diffractometer using $\text{CuK}\alpha$ radiation ($\lambda=1.5405 \text{ \AA}$). From the obtained data, crystallites sizes were determined using the width of the Ni (111) peak, after correcting for line-broadening^{16,17}.

Microhardness tests were conducted with a LECO micro-indenter model LM 247AT on both top as-received and metallurgically-prepared cross-sections of the electrodeposits, using a Vickers indenter with 10 and 25 g load (0.35 and 0.88 oz), respectively. Ten measurements were made for each load and the average is reported.

3. Results and discussion

3.1 Characterization of as-deposited Ni-W and Ni-W-P coatings

Table 2 shows the composition of Ni-W-P coatings as a function of NaH_2PO_2 added to the bath. W content diminishes as reverse current density increases, due to the preferential removal of elements with higher oxidation potential during the flow of a reverse current¹⁵. Semiquantitative chemical composition showed that the amount of P deposited could be controlled by

controlling the NaH_2PO_2 concentration in the bath. Similar results were found by Ahmad et al.¹⁸, who showed that for low concentration of 0.99 g/L (0.13 oz/gal), slight changes in concentration result in sharp changes in P content of deposited alloys whereas greater concentration saturates the P content in the coating. Table 2 shows that as the amount of deposited P increases the amount of Ni decreases up to 7% whereas the amount of deposited W decreases up to 96%. Concentrations of P lower than 0.5g/L (0.07 oz/gal) results in coatings with similar Ni-W ratios.

Table 2. Average compositions of deposited Ni-W-P coatings.

Sodium Hypophosphite in Bath [g/L]	P content [at. %]	W content [at. %]	Ni content I [at. %]
0	0	28.2	71.8
0.25	4.5	25.3	70.1
0.5	7.4	23.4	68.7
1	13.4	17.8	68.8
2	29.4	2.7	68.0
5	32.3	1.1	66.6

Figure 1 shows SEM micrographs of Ni-W-P coatings as a function of P concentration, it is clear that P causes differences in morphology with differences in composition. The spherical clusters observed in Ni-W appeared also in Ni-W-P coatings. The clusters grow with increasing NaH_2PO_2 concentration in bath up to 0.5 g/L (0.07 oz/gal). The size of clusters begins to decrease with higher concentrations. It is also important to mention that increasing P content in the bath caused a thinning of all coatings, as a result of a reduced rate of electrodeposition in agreement with previous studies^{13,18}.

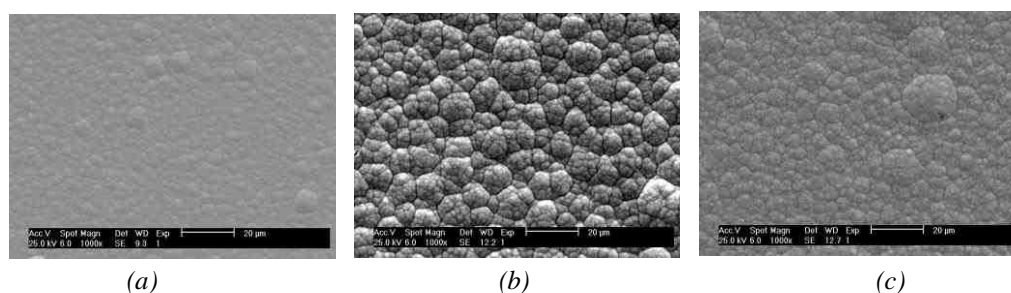


Figure 1. Surface SEM images of Ni-W-P coatings prepared with a) 0 g/L, b) 1g/L and c) 2g/L.

Figure 2 shows XRD pattern of Ni-W coatings as a function of P concentration. XRD of Ni (not shown here) revealed clearly that the addition of W causes a broadening of Ni peaks and a shift to lower angles. This is attributed to the reduction of average crystallite size and crystallinity together with the increase of W as an alloying element. This behavior agrees with the results of several other authors^{15,19-21}. Ni-W-P coatings prepared under the same conditions were also amorphous. XRD patterns show that the width of

the diffraction peaks increases with higher P and lower W content, which means that crystallinity decreases with increase in P content. In agreement with our findings, Ahmad et al.¹⁸ reported that the Ni-W coatings become completely amorphous when P content increases beyond ~ 5 at. %.

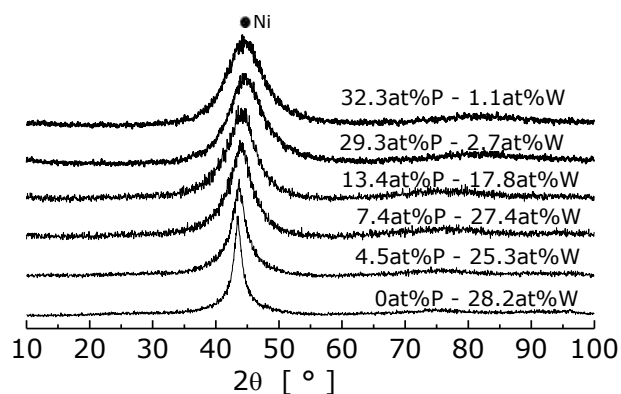


Figure 2. X-Ray Diffraction patterns obtained from as-deposited Ni-W coatings prepared as a function of P content.

Figure 3 shows the average grain size calculated from XRD pattern shown in Figure 2 as a function of P concentration in the bath. The crystallite size in Ni-W-P coatings decreases with increasing P content, which also results in a decrease in W content (Fig. 3).

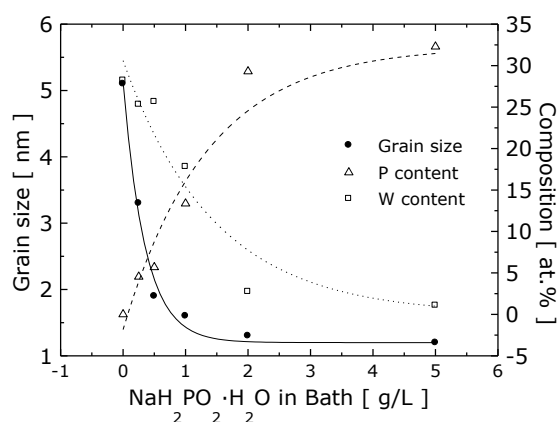


Figure 3. Effect of composition on crystallite size of Ni-W-P.

Figure 4 shows the microhardness of Ni-W-P coatings as a function of P content in the plating bath. Hardness ranged from 506 kgf/mm² for the lowest W content (1.1 W at. %) to 686 kgf/mm² for the highest W content (28.2 W at. %). In agreement with other authors, we found that coatings became harder with higher W content^{8,15,20,21}. This, again, should be attributed to the reduction in grain size favored by the presence of W. From these results, it is clear that P regulates W content in Ni-W coatings. Increasing the P content results in lowering W content (28.2-1.1 at. %),

decreasing grain size (6-1 nm), and decreasing the coating microhardness (686-506 kgf/mm²).

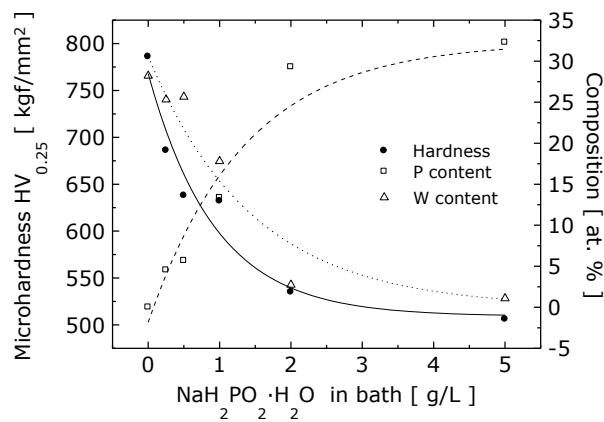


Figure 4. Effect of $\text{NaH}_2\text{PO}_2 \cdot \text{H}_2\text{O}$ concentration in plating bath on composition and microhardness of Ni-W-P coatings

Figure 5 shows the relationship between the inverse root of the apparent grain size and microhardness of all as-deposited Ni-W and Ni-W-P coatings. The graph shows that microhardness increases proportionally to the inverse of the square root of the grain size with increasing grain size up to a size of ~6 nm and then decreases proportionally with the square root of the grain size. The observed behavior at large grain sizes ($d > 6$ nm) follows the Hall-Petch relationship as expected^{22,23}. However, for small grain sizes an inverse Hall-Petch relationship is observed, in agreement with Ni-W and Ni-W-P materials^{18,19}.

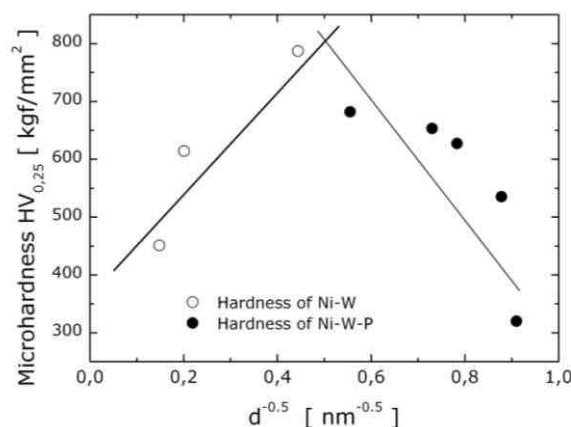


Figure 5. Relationship between apparent crystallite size and microhardness of as-deposited Ni-W-P coatings.

3.2 Characterization of the annealed Ni-W and Ni-W-P coatings

XRD patterns as a function of the concentration of NaH_2PO_2 in the plating bath are depicted in Figure 6. As annealing temperature increases, the crystallinity of the coating material increases and new phases appeared.

Furthermore, average crystallite sizes increase at increasing annealing temperature for all Ni-W-P samples.

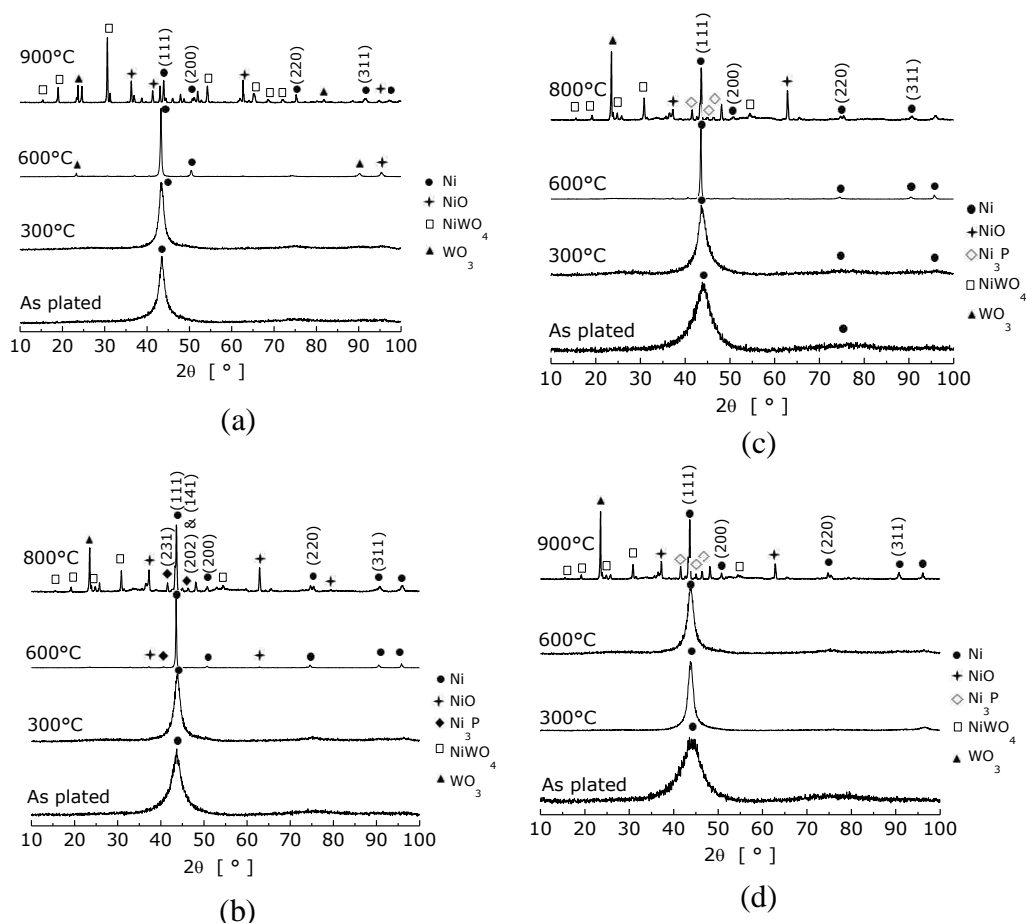


Figure 6. X-Ray Diffraction patterns for as-deposited and annealed samples of Ni-W-P coatings prepared with a) 0 g/L, b) 0.25 g/L, c) 0.5 g/L, and d) 1 g/L of $\text{NaH}_2\text{PO}_2 \cdot \text{H}_2\text{O}$.

Figure 6 shows that the width of the XRD peaks decreases with increasing annealing temperature and with decreasing phosphorus content. All samples annealed appear to be amorphous for annealing temperature below 300°C (572°F). Also, all samples annealed at higher temperatures, except for the one prepared with 1 g/L (0.134 oz/gal) of NaH_2PO_2 , are clearly crystalline.

Annealing at temperatures above 600°C (1112 °F) caused the formation of new phases in Ni-W-P coatings. Ni_3P peaks begin to appear at 600°C (1112 °F), and become sharper with increasing temperature. Several oxide phases were also detected with XRD. NiO peaks begin to appear at 600°C (1112 °F), and sharp NiWO_4 and WO_3 peaks appear at 800°C (1472 °F). In addition, it is important to note that, as previously observed in Ni-P coatings and Ni-P-W, the temperature of crystallization of electrodeposited coatings increases with increasing P content. Higher temperatures are needed

to crystallize Ni-W-P as P content increases. The same behavior was observed for Cr-C-P coatings¹³.

Figure 7 shows the dependence of the average crystallite size of Ni-W-P coatings as a function of annealing temperature. Clearly grain growth occurs during heat treatment, with grain sizes of Ni-W-P larger than those of Ni-W for temperature above 300°C (572 °F).

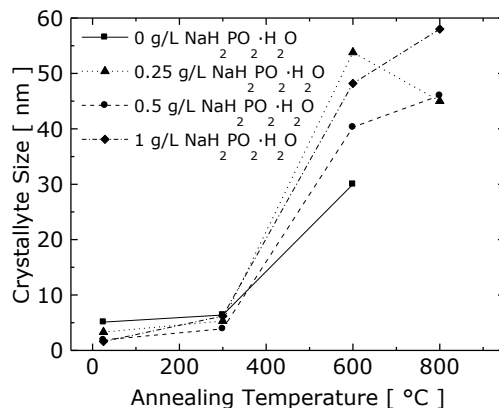


Figure 7. Effect of annealing on the average size of crystallites.

Figure 8 shows the effect of annealing temperature on the microhardness (measured at room temperature) of Ni-W and Ni-W-P coatings. The addition of P to the Ni-W electroplating bath and the consequent co-deposition of Ni-W-P has an important effect on the microhardness of the material. Even though at room temperature, the hardness of Ni-W-P is lower than that of Ni-W, we found that at higher temperatures the opposite is true. Furthermore, it should be noted that annealed Ni-W and Ni-W-P coatings reached higher hardness values than those obtained by conventional hard chromium coatings (full circles in Fig. 8) at annealing temperatures greater than 300°C (572 °F)¹³.

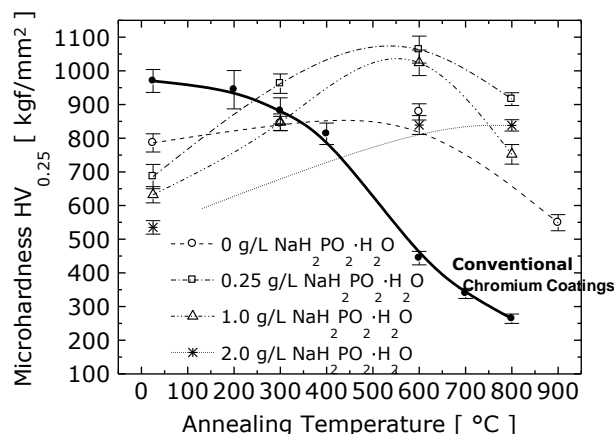


Figure 8. Effect of annealing on microhardness of Ni-W-P coatings.

Why does the incorporation of P to Ni-W coatings results in higher hardness with annealing temperatures? When no P is present as-deposited Ni-W coatings have the highest amount of W content (28 at. % W) and thus the smallest grain size and highest hardness value. However when P is present, its effect is more important than the effect of lowering the W concentration on the hardness behavior with increasing temperature.

The increase in microhardness with increasing annealing temperature should be attributed to the increasing crystallization of materials, resulting in the formation of a nanocrystalline alloy. The increased precipitation of the hard inter-metallic Ni₃P within grain boundaries of the Ni-W matrix avoids deformation and thus increases hardness. Since the amount of Ni₃P present increases with increasing annealing temperature, increased hardness could be attributed to increasing formation of this compound. This agrees with the behavior of electrodeposited multilayered Ni-W-P systems¹².

The decrease in hardness when annealing to 800°C (1472 °F) is attributed to the significant increase in grain size, which is explained by the Hall-Petch relationship²³. However, it is worth mentioning that since the grain size of Ni-W-P coatings does not increase significantly, its hardness only decreases slightly. Hardness of annealed Ni-W-P coatings with low P content (4.5 and 7.4 at. % P) did not show values below 856 kgf/mm², which are close to the highest value reached by Ni-W coatings. Thus, even though hardness of Ni-W-P begins to decay after 600°C (1112 °F), Ni-W-P coatings are still superior to Ni-W regarding the hardness dependence with annealing temperature.

Figure 8 also shows that hardness decreases with increasing P content for heat-treated and as-deposited coatings. This should be attributed to the decrease in crystallization with increasing P content, which can be clearly observed in the XRD patterns of Ni-W-P (Fig. 7). This effect may be attributed to the fact that P is increasing the crystallization temperature of the material, as reported for other systems¹³.

4. Conclusions

During this work we studied the physicochemical and mechanical properties of Ni-W-P coatings electrodeposited onto steel by pulsed current as a function of P content and annealing temperatures. Specifically the main conclusions extracted from this study can be summarized as follow:

1. The addition of P to the Ni-W electroplating bath leads to the co-deposition of Ni-W-P and the sodium hypophosphite concentration controls the deposition of P.
2. Microhardness values of the as-deposited Ni-W-P coatings are lower than those corresponding to Ni-W coatings.
3. Annealing causes Ni-W-P coatings to reach hardness values (up to ~1050kgf/mm²) greater than those reached by as-deposited and annealed Ni-W coatings. This is attributed to the Ni₃P within grain boundaries of the Ni-W matrix.

4. Increasing P content decreases the hardness of the annealed coatings. We attribute this to the fact that P increases the crystallization temperature of the materials.

5. References

- ¹ B. Li, A. Lin & F. Gan, *Surface and Coating Technology* **201**, 2578-2586, (2006).
- ² G.J. Sargent, *Trans. Am. Electrochem. Soc.*, **37**, 479-497, (1920).
- ³ C.G. Fink, US Patent N° 1,581,188, (1926).
- ⁴ J.P. Hoare, *J. Electrochem. Soc.* **126**(2), 190-199, (1979).
- ⁵ G.A. Lausmann, *Surface and Coatings Technology*, **86-87**, 814-820, (1996).
- ⁶ I. Shuker & K.R. Newby, *Transactions of the Institute of Metal Finishing*, **83** (6), 272-274, (2005).
- ⁷ E.W. Brooman, *Proc. AESF SUR/FIN '05*, (2005).
- ⁸ W.-S. Hwang & J.-J. Lee, *Materials Science Forum*, **510-511**, 1126-1129, (2006).
- ⁹ N. Eliaz, T.M. Sridhar, & E. Gileadi, *Electrochimica Acta*, **50**, 2893-2904, (2005).
- ¹⁰ S.-K. Tien, J.-G. Duh, & Y.-I. Chen, *Surface and Coatings Technology*, **177-178**, 532-536, (2004).
- ¹¹ C.N. Panagopoulos, V.D. Papachristos, U. Wahlstrom, P. Leisner, and L.W. Christoffersen, *Scripta Materialia*, **43**, 677-683, (2000).
- ¹² V.D. Papachristos, C.N. Panagopoulos, U. Wahlstrom, L.W. Christoffersen, P. Leisner, *Materials Science and Engineering*, **A279**, 217-230, (2000).
- ¹³ M.J.L. Gines, F.J. Williams, & C.A. Schuh, *Metallurgical and Materials Transactions*, **A 38**, 1367-1370, (2007).
- ¹⁴ C.A. Schuh, US Patent Application 20060272949.
- ¹⁵ A.J. Detor, C.A. Schuh, *Acta Materialia*, **55**, 371-379, (2007).
- ¹⁶ H.P. Klug & L.E. Alexander, "X-ray diffraction procedures", 2nd Edition, John Wiley & Sons, (1974).
- ¹⁷ Z. Zhang, F. Zhou, & E.J. Lavernia, *Metallurgical and Materials Transactions*, **A 34**, 1349-1355, (2003).
- ¹⁸ J. Ahmad, K. Asami, A. Takeuchi, & A. Inoue, *Materials Transactions*, **44** (4), 705-708, (2003).
- ¹⁹ T. Yamasaki, P. Schobmacher, K. Ehrlich, & Y. Ogino, *Nanostructured Materials*, **10**(3), 375-388, (1998).
- ²⁰ T. Yamasaki, R. Tomohira, Y. Ogino, P. Schobmacher, & K. Ehrlich, *Plating and Surface Finishing*, **87**, 148-152, (2000).
- ²¹ T. Yamasaki, *Mater. Phys. Mech.*, **1**, 127-132, (2000).
- ²² C.A. Schuh, T.G. Nieh, & H.Iwasaki, *Acta Mat.*, **51**, 431-443, (2003).

²³ S.C. Tjong & H. Chen, *Materials Science and Engineering*, **R45**, 1-88, (2004).